Solid Light Concentrators for Cherenkov Astronomy

Isabel Braun*, **Luisa Sabrina Stark***, **Michael Backes**[x], **Adrian Biland***, **Andrea Boller***, **Thomas Bretz**[‡], **Sebastian Commichau***, **Volker Commichau***, **Daniela Dorner**[*§], **Arno Gadola**[¶], **Hanspeter von Gunten***, **Adamo Gendotti***, **Oliver Grimm***, **Dorothée Hildebrand***, **Urs Horisberger***, **Ben Huber**[¶], **Thomas Krähenbühl***, **Daniel Kranich***, **Eckart Lorenz**[*‖], **Werner Lustermann***, **Karl Mannheim**[‡], **Dominik Neise**[§], **Felicitas Pauss***, **Dieter Renker****, **Wolfgang Rhode**[x], **Michael Rissi***, **Sebastian Rollke**[x], **Ulf Röser***, **Stefan Steiner**[¶], **Ulrich Straumann**[¶], **Jean-Pierre Stucki***, **Gert Viertel***, **Patrick Vogler***, **Achim Vollhardt**[¶] **and Quirin Weitzel***

**Institute for Particle Physics, ETH Zurich, 8093 Zurich, Switzerland*
[x]TU Dortmund University, 44221 Dortmund, Germany
[‡]University of Würzburg, 97074 Würzburg, Germany
[§]ISDC Data Center for Astrophysics, University of Geneva, 1290 Versoix, Switzerland
[¶]University of Zurich, 8057 Zurich, Switzerland
[‖]Max Planck Institute for Physics, 80805 Munich, Germany
***Paul Scherrer Institute, 5232 Villigen, Switzerland*

Abstract. **Pixelized cameras of Imaging Atmospheric Cherenkov Telescopes use hollow light guides with reflective surfaces based on the Winston cone design. These cones minimize insensitive spaces between the photo sensors and shield the camera from stray background light by limiting the angular acceptance to the primary reflector area. Raytracing simulations comparing different geometries and materials were performed. Especially in combination with the favourable angular acceptance properties of Geiger-mode Avalanche Photodiodes as used in the FACT Project, these simulations show that solid cones based on total reflection allow larger concentration ratios than the classical hollow cones for the price of additional background light. Simulation results for different geometries and test measurements with hollow and glass cones will be presented.**

***Keywords*: Solid Winston cones, Cherenkov Telescopes, FACT**

I. Introduction

Light guides serve a double purpose: they enlarge the sensitive area, filling possible dead spaces between the photon detectors and shield the sensors from stray light with large incidence angles. They are usually installed directly in front of the camera's photo sensors.

Several wall shapes have been studied, the most successfull being the compound parabolic concentrator (CPC) described by R. Winston *et al.* (see e.g.[1]). The walls of this type of light guide, often called ”Winston cone”, follow a tilted parabolic shape. Incindent rays with a predefined limiting angle Φ are reflected to the opposite edge of the exit apparture in one single reflection. Rays with incidence angles θ smaller than Φ are reflected onto the exit area, while larger incidence angles are rejected by back-reflection on the opposite surface. This creates a sharp cutoff in efficiency at the limiting angle, ideal for the purposes defined above. The limiting angle is chosen to match the f/D ratio of the telescope so that the light sensor of each concentrator ”sees” only the complete primary reflector with optimum efficiency. While a Whipple[2]-style telescope with $f/D = 0.7$ requires a limiting angle $\Phi = \tan^{-1}(D/2f) = 35.5°$, the angle reduces to 22.6° and even 15.5° for $f/D = 1.2$ (e.g. H.E.S.S. [3], possibly DWARF[4]) or 1.8 (possibly CTA [5]) respectively.

Defining the concentration factor as the ratio between input and output area of a light guide, the maximum possible concentration factor C_{max} for an axisymmetric concentor is [1]

$$C_{max} = (\frac{1}{\sin\Phi})^2, \qquad (1)$$

i.e. 5.0 for telescopes with an f/D of 1 (e.g. MAGIC [6], $\Phi = 26.6°$) or 9.9 for an f/D of 1.5 (alternative for CTA, $\Phi = 18.4°$).

Other shapes with parabolic or the more easily manufactured flat walls show a softer cutoff in the efficiency curve. By that, more stray light, usually coming from the isotropic night sky background (NSB), is allowed to reach the camera. These shapes deviating from the CPC design in general need more reflections to transport the light through the concentrator. Increasing their length sharpens the cutoff edge, but leaves its position unchanged until reflectivity losses are dominant. Therefore, these shapes become interesting mainly for highly reflective surfaces.

II. Simulations

Ray tracing simulations were performed to study the behaviour of varying shapes and to optimize the cone

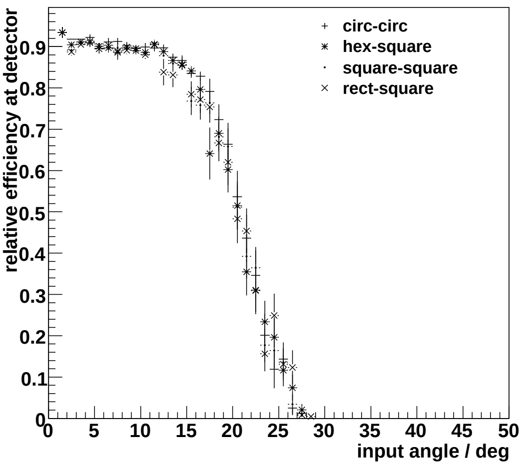

Fig. 1: Comparison of parabolic concentrators with different input and output shapes, but the same concentration factor of 6.6. The first phrase in the legend denotes the shape of the input area, the second phrase the output area (circ=circular, hex=hexagonal, square=quadratic and rect=rectangular shape).

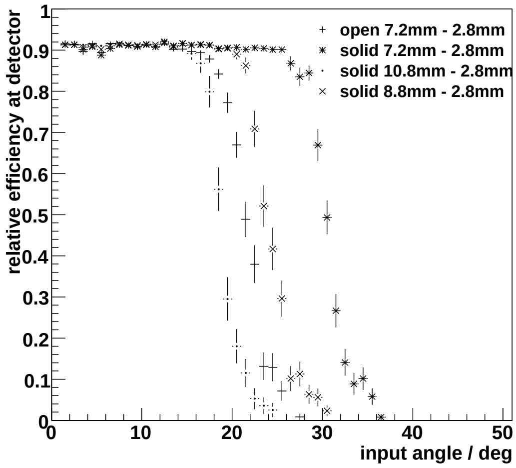

Fig. 2: Comparison of an open and solid CPC ($n = 1.5$) with an area concentration factor $C = 6.6$, as well as solid CPCs with $C = 14.9$ and $C = 9.9$. 5% reflection losses were assumed for both types. Error bars are purely statistical and indicate variations caused by different input points on the entrance area and different directions ϕ.

for a given purpose, in this case being used in the G-APD based camera FACT [7] intended for the DWARF telescope [4].

In each simulation, a large number of rays with randomized input direction (θ, ϕ) and position are tracked through the light guides and subsequently through the detector geometry. In each reflection, the relative intensity of the ray is reduced according to the reflectivity of the wall until the ray leaves the cone through either opening. Additionally, absorption losses within different media, refraction and Fresnel reflection are implemented. For the G-APDs used in the FACT project, the sensitive silicon surface is protected by a resin layer of up to 0.45 mm thickness (typically ~ 0.3 mm), allowing some rays with large output angles to miss the detector. Hence, ray tracing is continued until the level of the active surface is reached. In contrast to traditional photomultiplier tubes, the acceptance of G-APDs is homogeneous both in incidence angle (measurements show flat acceptance for angles up to at least 80°) and space (in fact, homogeneous illumination of the active surface is desired to reduce sensitivity losses caused by cell occupancy) [9].

In Cherenkov astronomy, equidistant pixels (on a hexagonal grid) are favoured, therefore hexagonal entrance areas are a natural choice. However, rectangular shapes are equally possible and easier to manufacture.

For parabolic walls, no significant difference in the acceptance curves can be detected between cones with circular input and output areas and those with hexagonal, quadratic or rectangular (side ratio: $\sqrt{3}/2$) input and quadratic output area if they have the same area concentration factor (see Fig. 1).

III. Solid Concentrators

Solid concentrators [8] are filled with a dielectric medium and are typically based on total reflection. Their principal differences to open cones arise from the primary refraction: rays are traced through the cone as if they had smaller incidence angles. This leads to a larger NSB contribution compared to an open cone of the same geometry, but also to the possibility of larger area concentration ratios.

The maximum theoretical concentration ratio for solid CPCs depends on the refractive index n_M of the used material, which is best chosen to match the refractive index of the light sensor protection (resin with $n \sim 1.5$). If close optical contact is achieved, the maximum theoretical CPC concentration for 3D concentrators is increased by a factor of n_M^2 [1]. From the simulations, this seems to match if only the transmission through the cone is considered. However, once the acceptance of the detector is included, an increase by a factor between n_M and n_M^2 seems more realistic (see Fig. 2).

Total reflection is theoretically 100% efficient, but the effects of a finite surface roughness (see below) lead to light losses when the condition for total reflection is locally not fulfilled.

IV. Prototype Measurements

Measurements on the angular acceptance of two types of light guide prototypes were performed. Both prototypes have a simple pyramidical shape with quadratic input and output areas. For both cases, the input area measures $7.2\times7.2\,\mathrm{mm}^2$ and the exit area $2.8\times2.8\,\mathrm{mm}^2$. The length is 20 mm for the open and 25 mm for the

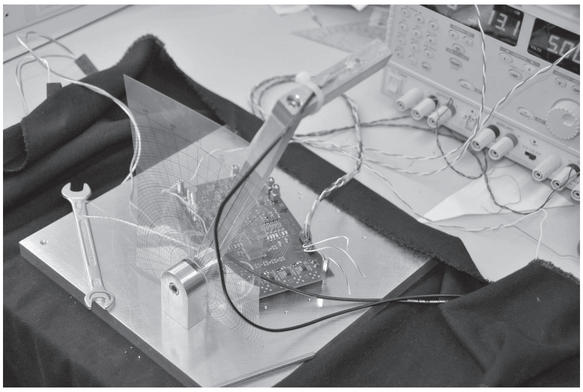

Fig. 3: Setup to measure the angular efficiency of the light concentrators. A pulsed LED is mounted on the metal bar in the foreground. The angle relative to the vertical direction can be read from a transparent angular scale. This lever is mounted on a common base plate with the board holding G-APDs, electronic amplification and light guides. Special holes in the base plate allow measuring selected input orientations (parallel to a G-APD edge or to the diagonal).

solid concentrator. The open concentrator is made of an Aluminum frame with Vikuiti ESR foil (reflectivity 98%, specified by the manufacturer 3M) as reflector. The solid concentrator is made of cut and polished UV-transparent glass (Schott N-FK5). A unit formed of four concentrators is attached to four G-APDs (sensitive area $3.0{\times}3.0\,\mathrm{mm}^2$ each), the added signal of which is read out. A pulsed LED was rotated around the entrance plane (see Fig. 3).

Surface Roughness

Fig. 4 shows a comparison between simulations and the (rescaled) measurements for both prototypes and light incident along a G-APD edge (Fig. 4a, $\phi = 0°$) or the diagonal (Fig. 4b, $\phi = 45°$). The visible excess of measured light at large input angles could not be attributed to residual stray light or signal non-linearities. It applies to both cone types.

The simulation was extended to include a measure for the variable surface roughness. It is implemented as a random addition and subtraction of material along the normal direction up to a maximum of $d\zeta$ over a distance of $d\xi$ along the surface. A value of $d\zeta : d\xi$ = 1:1 corresponds to peaks and valleys changing the slope by up to 45°. Figure 5 shows the angular acceptance of three simulated pyramidic cones with different roughness. In these simulations, the angle ϕ was fixed to match the measurements. G-APD noise (measured in the dark) was subtracted from the measured data points, and they are renormalized. The collection and shielding power of the light guides degrade with increasing surface roughness. A simulated roughness of 0.5:1 is in very good agreement with the measurements for both cone types.

V. Summary and Outlook

Solid cones are especially suited for future G-APD applications in Cherenkov astronomy, increasing the effective area for relatively small cost. Further properties specific to solid cones being studied:

- optical crosstalk between neighbouring pixels: light rejected because of the limiting angle for total reflectivity could enter another cone and be detected by the wrong pixel.
- the track of scintillation light from local muons traversing the cones could lead to false triggers. At certain angles, the resulting line pattern could be mistaken for shower images.

Effects of the surface roughness can not be neglected for any type of light concentrator. Measurements of prototypes made from UV-transparent Plexiglas will soon be shown. A comparative study of surface qualities achieved with different fabrication techniques is planned. Special focus lies on molding, since it is ideal for mass production.

References

[1] R. Winston, J.C. Minano, P. Benitez, *Nonimaging Optics*, Elsevir Academic Press, 2005.
[2] T. C. Weekes *et al.* , *Observation of TeV gamma rays from the Crab nebula using the atmospheric Cerenkov imaging technique*, Astrophys. Journal **342**, 379-395, 1989.
[3] H.E.S.S. collaboration, *official homepage*, http://www.mpi-hd.mpg.de/hfm/HESS/
[4] T. Bretz *et al.* , *Long-term VHE gamma-ray monitoring of bright blazars with a dedicated Cherenkov telescope*, in these proceedings.
[5] Cherenkov Telescope Array, *official homepage*, http://www.cta-observatory.org
[6] MAGIC collaboration, *official homepage*, http://magic.mpp.mpg.de
[7] Q. Weitzel *et al., A Novel Camera Type for Very High Energy Gamma-Astronomy*, in these proceedings.
[8] R. Winston, *Dielectric Compound Parabolic Concentrators*, Appl. Opt. **15** 291-292, 1976.
[9] T. Krähenbühl *et al., Geiger-mode Avalanche Photodiodes as Photodetectors in Cherenkov Astronomy*, in these proceedings.

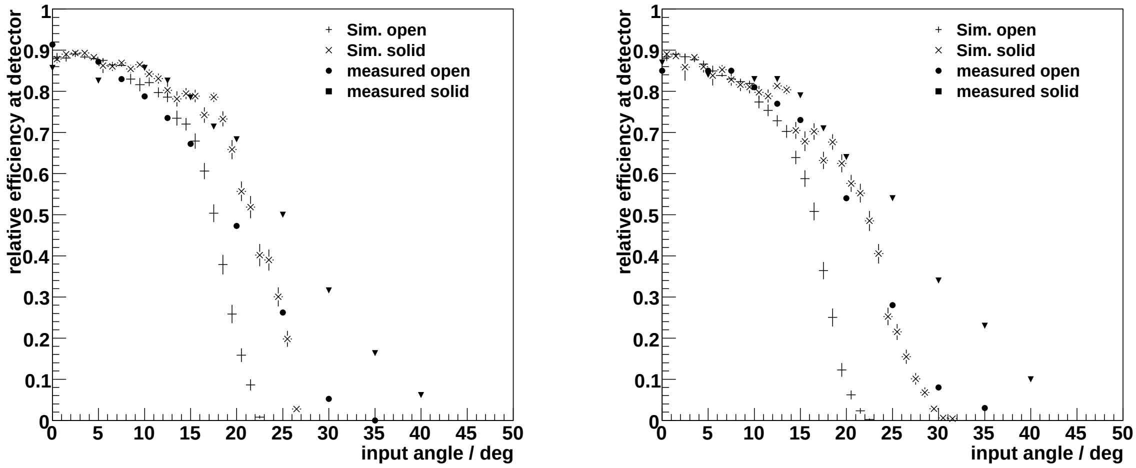

(a) $\phi = 0°$ (b) $\phi = 45°$

Fig. 4: Comparison between simulated angular acceptance curves and measurements (rescaled) for pyramidic cones. Two input directions ($\phi = 0°$ and $\phi = 45°$) were measured for each prototype.

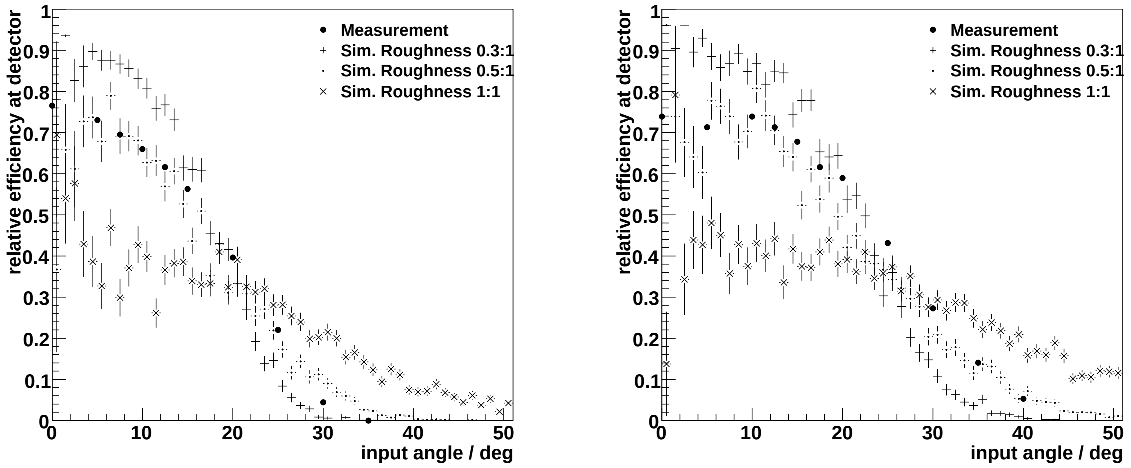

(a) Open cones (b) Solid cones

Fig. 5: Angular acceptance curves for different surface roughness (0.3:1, 0.5:1, 1:1) for pyramidic cones compared to measurements (rescaled).